NUCLEAR INSTRUMENTS AND METHODS 105 (1972) 565–572; © NORTH-HOLLAND PUBLISHING CO.

# ELECTROSTATIC PROBLEMS IN MULTIWIRE PROPORTIONAL CHAMBERS

G. A. ERSKINE

*CERN, Geneva, Switzerland*

Received 10 July 1972

Starting from the known complex potential of an infinite grid of thin wires lying between parallel grounded electrodes, the following problems are discussed: 1) the electrostatic coupling between wires, 2) the effect of varying the diameter of a single wire, 3) the effect of displacing a single wire. Figures are given which show the magnitude of these effects for a symmetric chamber of arbitrary dimensions. The computer generation of field plots for proportional chambers is briefly discussed.

## 1. Introduction

A multiwire proportional chamber[1]) consists of a plane grid of equally spaced wires lying between, and parallel to, a pair of plane grounded electrodes. Each wire is connected to its own unidirectional amplifier, and is maintained at a constant positive potential. If a charged particle traverses the grid, an electron avalanche is produced in the ionizable gas with which the chamber is filled, causing a negative pulse to appear on the nearest wire.

Since the distance between the plates is, in practice, very much less than the height or width of the chamber, the electrostatic configuration may be regarded as two-dimensional. Choosing a $z$-plane coordinate system in which the electrodes are situated at $y = \pm L$, the complex potential at an arbitrary point $z$ arising from a *single* line charge of unit strength situated at $z'$ is (ref. 2, p. 90):

$$\phi(z,z') = -2\ln\left\{\frac{\sinh[(\pi/4L)(z-z')]}{\cosh[(\pi/4L)(z-\bar{z}')]}\right\}, \qquad (1)$$

where $\bar{z}'$ is the complex conjugate of $z'$. The corresponding physical potential at $z$ is

$$v(z,z') = \mathrm{Re}[\phi(z,z')].$$

If the line charge at $z' = x' + \mathrm{i}y'$ represents a wire of radius $r = \frac{1}{2}d$, where $r \ll L$, the physical potential of a point on the wire will be denoted by $v(z', z')$, where

$$v(z',z') = -2\ln\left\{\frac{\pi d/8L}{\cos(\pi y'/2L)}\right\}. \qquad (2)$$

For an infinite grid of unit line charges with spacing $s$ (fig. 1) situated at $z_k = z_0 + ks$, $k = 0, \pm 1, \pm 2, \ldots$, the complex potential $\psi(z)$ may be obtained by summing $\phi(z, z_k)$ from $k = -\infty$ to $k = +\infty$. This leads to a computationally convenient expression in terms of theta functions[2]). Alternatively, the potential may be derived directly from the appropriate array of image charges, leading to an expression in terms of Jacobian elliptic functions[3]). Transforming the expression (ref. 2, p. 93) to the coordinate system defined above, using a known relation[4]) between the functions $\vartheta_1$ and $\vartheta_4$, and neglecting an additive constant equal to $\mathrm{i}\pi$, we obtain

$$\psi(z) = \mathrm{i}\,\frac{2\pi y_0}{Ls}(z-x_0) - 2\ln\left\{\frac{\vartheta_1[(\pi/s)(z-z_0)|\mathrm{i}4L/s]}{\vartheta_4[(\pi/s)(z-\bar{z}_0)|\mathrm{i}4L/s]}\right\}. \qquad (3)$$

The complex potential for a *symmetric* chamber is obtained by setting $z_0 = x_0 + \mathrm{i}y_0 = 0$:

$$\psi_{\mathrm{S}}(z) = \frac{2\pi L}{s} - 2\ln\left[\frac{2(\sin\zeta - q^2\sin 3\zeta + q^6\sin 5\zeta - \ldots)}{1-2(q\cos 2\zeta - q^4\cos 4\zeta + q^9\cos 6\zeta - \ldots)}\right], \qquad (4)$$

where $\zeta = \pi z/s$ and $q = \exp(-4\pi L/s)$. The term $2\pi L/s$ arises from a factor $q^{\frac{1}{4}}$ which is present in the definition of $\vartheta_1$, but not in $\vartheta_4$.

In practice $L > s$, and $q$ is therefore a small quantity. Neglecting $q$ in eq. (4) gives the following approximate potential:

$$\psi_{\mathrm{S}}(z) \approx (2\pi L/s) - 2\ln[2\sin(\pi z/s)]. \qquad (5)$$

The corresponding physical potential is the real part of this:

$$V_{\mathrm{S}}(z) \approx (2\pi L/s) - \ln[4\sin^2(\pi x/s) + 4\sinh^2(\pi y/s)] \qquad (6)$$

– an approximation which can also be obtained[1]) from the potential of an infinite grid in free space by adding a constant so chosen as to make the real potential vanish at $z = ks \pm iL$. If $\Delta L$ is the maximum deviation of the $V=0$ equipotential given by eq. (6) from the lines $y = \pm L$, we have $|\Delta L/L| = (s/\pi L)\exp(-2\pi L/s)$, a quantity which is equal to $6\times 10^{-4}$ when $L/s = 1$, and to $6\times 10^{-7}$ when $L/s = 2$. Approximations (5) and (6) may therefore be used even when $L/s$ is of order unity.

In order to calculate the charge $Q$ per unit length on each wire of diameter $d = 2r$, we assume that, for $|z| = r$, $\sin(\pi z/s)$ in eq. (5) may be replaced by $\pi z/s$. This approximation effectively replaces a slightly elliptical equipotential by an exactly circular one, where the maximum distance $\Delta r$ between the two is given by $|\Delta r/r| = \frac{1}{6}(\pi r/s)^2$, equal to $4\times 10^{-5}$ when $d/s$ has the typical value 0.01. Using this approximation and setting $\mathrm{Re}[Q\psi_S(r)] = V_0$, where $V_0$ is the grid potential, gives

$$Q = \frac{V_0}{(2\pi L/s) - 2\ln(\pi d/s)}.$$

The field intensity at any point $z$ is given by $E = E_x + iE_y = -\overline{Q\psi'(z)}$. Therefore, using eq. (5), the magnitude of the field intensity in a symmetric chamber is

$$|E| = Q\,|\psi_S'(z)| = (2\pi Q/s)\,|\cot(\pi z/s)|.$$

Fig. 2 shows the relationship between $|E|$ and $|z|$ for real $z$ and pure imaginary $z$. The field $2Q/|z|$ corresponding to an isolated line charge is also shown for comparison. It can be seen that the region around each wire within which the field is effectively isotropic extends to approximately $0.1\,s$.

## 2. Electrostatic coupling between wires

As a result of electrostatic coupling between the wires, the negative pulse which appears on a wire when it collects an avalanche should be accompanied by induced negative pulses on the nearby wires. This effect, if dominant, would interfere with the exact localization of the wire collecting the avalanche; and it was at one time considered necessary to place one or more screening wires between each pair of active wires to reduce the electrostatic coupling. In practice, however, the pulses which appear in the chamber are caused mainly by the motion of the sheath of positive ions in the strong field around the collecting wire. This motion, which is in fact the main cause of the negative pulse on the collecting wire, produces *positive* pulses on the remaining wires[1]). These positive pulses have an amplitude which is much greater than that of the negative pulses induced electrostatically. The sum of the two contributions is therefore a positive pulse which is easily rejected by the use of unidirectional amplifiers.

The magnitude of the electrostatic coupling between the wires is of practical interest for calculations concerning the induced pulses. To calculate this coupling we consider a chamber in which wire 0 is isolated and raised to a potential $\Delta V$, while the electrodes and the remaining wires are maintained at zero potential. If the resulting charge on the $j$th wire is denoted by $\Delta q_j$, $j = 0, \pm 1, \pm 2, \ldots$, the coupling capacitance between wire 0 and wire $j$ is equal to $c_j = \Delta q_j/\Delta V$.

The physical potential at a point $z$ is given by

$$V(z) = \sum_{j=-\infty}^{\infty} \Delta q_j\, v(z, z_j),$$

and we require that $V(z)$ shall have the value $\Delta V$ on the surface of wire 0 and shall vanish at $z = z_k$ for $k \neq 0$.

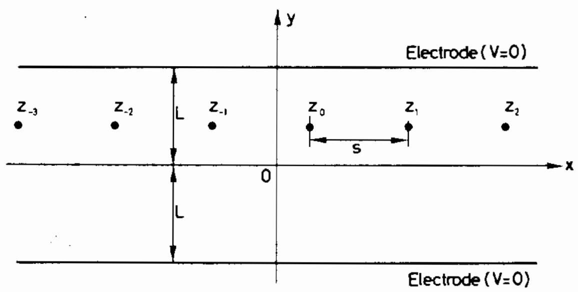


Fig. 1. Coordinate system.

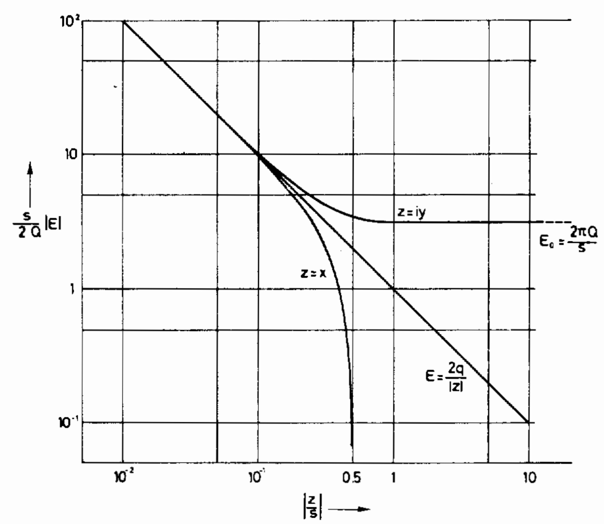


Fig. 2. Field intensity $|E| = (2\pi Q/s)|\cot(\pi z/s)|$ along the $x$ and $y$ axes of a symmetric chamber. The field $E = 2Q/|z|$ of an isolated line charge is shown for comparison.

On defining $\delta_{k0}$ to be the Kronecker symbol (equal to 1 if $k=0$, otherwise zero), these conditions lead immediately to the following system of simultaneous equations determining the $c_j$:

$$\sum_{j=-\infty}^{\infty} a_{k-j}\, c_j = \delta_{k0}\,, \tag{7}$$

where $a_{k-j} = v(z_k, z_j)$ depends only on the difference $k-j$, and where $a_0 = v(z_k, z_k)$ is the real potential at distance $\frac{1}{2}d$ from a unit line charge at $z_k$. For a symmetric chamber, using eqs. (1) and (2),

$$\begin{aligned} a_0 &= -2\ln(\pi d/8L), \\ a_m &= -2\ln|\tanh(m\pi s/4L)|, \quad \text{for } m \neq 0. \end{aligned} \tag{8}$$

The solution of equations of the form (7) is discussed in the appendix. Fig. 3 shows the quantities $c_j$ (which are dimensionless in the electrostatic units used here) as functions of $L/s$ for a symmetric chamber. The capacitance per unit length in units of pF/m may be obtained by multiplying by $1.1\times10^2$. The full lines in the figure correspond to $d/s=0.01$, and the short segments at each end to $d/s=0.005$ and $d/s=0.02$. The dependence on $L/s$ is much greater than on $d/s$. The figure shows that the coupling capacitance between any two wires decreases as $L/s$ decreases, since a wire ceases to 'see' its neighbours if they are much further away than the electrodes. On the other hand, the self-capacitance of a single wire, as measured by $c_0$, has a value (10 pF/m) which is almost independent of the dimensions of the chamber.

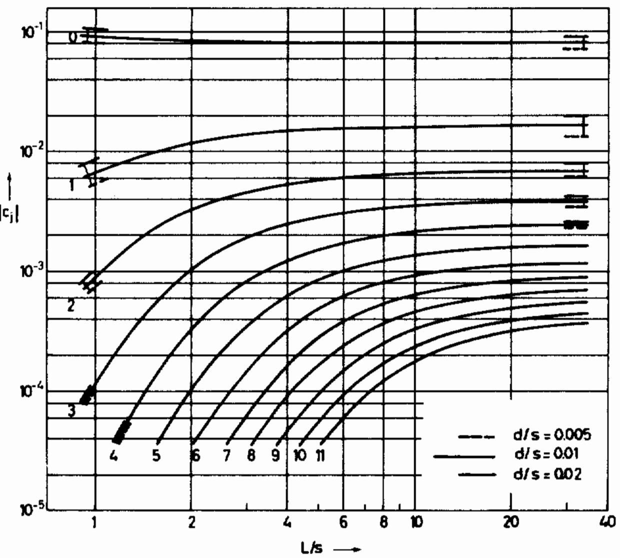


Fig. 3. Coefficients $c_j$ (negative if $j\neq0$) for a symmetric chamber. Coupling capacitance between wires 0 and $j$ is $1.1\times10^2 c_j$ pF/m. Diameter variation coefficient is $e_j = 2c_j$.

## 3. The effect of varying the diameter of a single wire

The extent to which the field in a multiwire chamber will be perturbed by fluctuations in wire diameter can be estimated by considering an idealized situation in which only one wire has a diameter differing from the nominal value. We suppose therefore that wire 0 has diameter $d+\Delta d$, but that all other wires have diameter $d$. If $\Delta q_j$ are the corresponding perturbation charges, the physical potential at a point $z$ is given by

$$V(z) = \sum_{j=-\infty}^{\infty} (Q+\Delta q_j)\, v(z, z_j).$$

The imposed conditions are that $V(z_k) = V_0$ for all $k$. For $k\neq0$, $v(z_k, z_k)$ is to be interpreted as the potential at distance $\frac{1}{2}d$ from a unit line charge at $z_k$; but $v(z_0, z_0)$ is to be interpreted as the potential at distance $\frac{1}{2}(d+\Delta d)$ from $z_0$. Therefore, using eqs. (8) and (2),

$$\begin{aligned} v(z_k, z_j) &= a_{k-j}, \quad \text{for } k\neq 0 \text{ or } j\neq 0, \\ v(z_0, z_0) &= a_0 - 2\ln(1+\Delta d/d) \\ &\approx a_0 - 2(\Delta d/d). \end{aligned}$$

Using $Q\sum_j v(z_k, z_j) = V_0$, the equations for the $\Delta q_j$ become

$$\sum_j a_{k-j}\,\Delta q_j = 2\delta_{k0}(Q+\Delta q_0)(\Delta d/d). \tag{9}$$

Since $\Delta q_0/Q$ tends to zero as $\Delta d/d$ tends to zero, $\Delta q_j/(Q+\Delta q_0)$ approaches $\Delta q_j/Q$. Therefore, on defining

$$e_j = \frac{(\Delta q_j/Q)}{(\Delta d/d)},$$

the eqs. (9) take the following form when $\Delta d/d$ is small:

$$\sum_j a_{k-j}\, e_j = 2\delta_{k0}\,.$$

These equations differ from eqs. (7) of section 2 only by the presence of a factor 2 on the right-hand side. Therefore $e_j = 2c_j$, where the $c_j$ are the solutions of eq. (7) as shown in fig. 3. The coefficients $e_j$ measure the sensitivity of the charge on wire $j$ to variations in the diameter of wire 0. As is to be expected, this sensitivity is greatest for wire 0 itself, with $(\Delta q_0/Q)\approx 0.2(\Delta d/d)$ irrespective of the dimensions of the chamber.

## 4. The effect of displacing a single wire

We shall now consider a chamber in which wire 0 has been displaced from $z_0$ to $z_0+\Delta z$, where $\Delta z$ is finite, while the other wires remain at $z_k = z_0+ks$, $k = \pm 1, \pm 2, \ldots$ Introducing perturbation charges $\Delta q_j$, the physical potential at a point $z$ is given by

$$V(z) = \sum_{j\neq 0} (Q+\Delta q_j)\, v(z, z_j) + (Q+\Delta q_0)\, v(z, z_0+\Delta z).$$

With our usual convention that $v(z', z')$ denotes the real potential at distance $\frac{1}{2}d$ from a unit line charge at $z'$, we define

$$\begin{aligned} f_0(\Delta z) &= v(z_0, z_0) - v(z_0+\Delta z, z_0+\Delta z), \\ f_k(\Delta z) &= v(z_0, z_k) - v(z_0+\Delta z, z_k) \\ &= v(z_k, z_0) - v(z_k, z_0+\Delta z), \quad \text{for } k \neq 0, \\ a_{k-j} &= v(z_k, z_j), \\ u_j &= \Delta q_j/Q. \end{aligned}$$

The requirement that $V(z_0+\Delta z) = V_0$ and that $V(z_k) = V_0$ for $k \neq 0$, together with the equation $Q\sum_j v(z_k, z_j) = V_0$, yields

$$\sum_{j=-\infty}^{\infty} a_j u_j = \sum_{j=-\infty}^{\infty} (1+u_j) f_j(\Delta z),$$
$$\sum_{j=-\infty}^{\infty} a_{k-j} u_j = (1+u_0) f_k(\Delta z), \quad \text{for } k \neq 0. \tag{10}$$

If the terms involving $u_j$ are all brought to the left-hand side, the coefficient matrix is no longer merely equal to $a_{k-j}$ as in eq. (7), but has been modified in its zeroth row and zeroth column. However, as is shown in the appendix, the problem may be reduced to one involving only the unmodified matrix $a_{k-j}$.

When the displacement $\Delta z = \Delta x + i\Delta y$ is small, the essential information is contained in the leading coefficients of the Taylor's series expansion of $u_j$ in powers of $\Delta x$ and $\Delta y$. The expansion for $j = 0$ contains only even powers of $\Delta x$, since $\Delta q_0$ is unaffected by a reversal in the sign of $\Delta x$; but the expansion for $j \neq 0$ contains both even and odd powers of $\Delta x$. Similarly, if the chamber is symmetric, only even powers of $\Delta y$ can be present for any $j$, since $\Delta q_j$ is independent of the sign of $\Delta y$. Therefore, for a symmetric chamber,

$$\Delta q_j/Q = a_1(\Delta x/s) + a_2(\Delta x/s)^2 + b_2(\Delta y/s)^2 + \ldots,$$

where the coefficients $a_1, a_2, b_2, \ldots$ depend on $j$, and where $a_1 = 0$ if $j = 0$. For $j \neq 0$, the second term can be neglected in comparison with the first, so that the realistic approximations are

$$\Delta q_0/Q \approx a_2^{(0)}(\Delta x/s)^2 + b_2^{(0)}(\Delta y/s)^2,$$
$$\Delta q_j/Q \approx a_1^{(j)}(\Delta x/s) + b_2^{(j)}(\Delta y/s)^2, \quad \text{for } j \neq 0.$$

A direct method for the calculation of these coefficients is outlined in the appendix. Figs. 4 and 5 show their values as functions of $L/s$ for $d/s = 0.01$, with

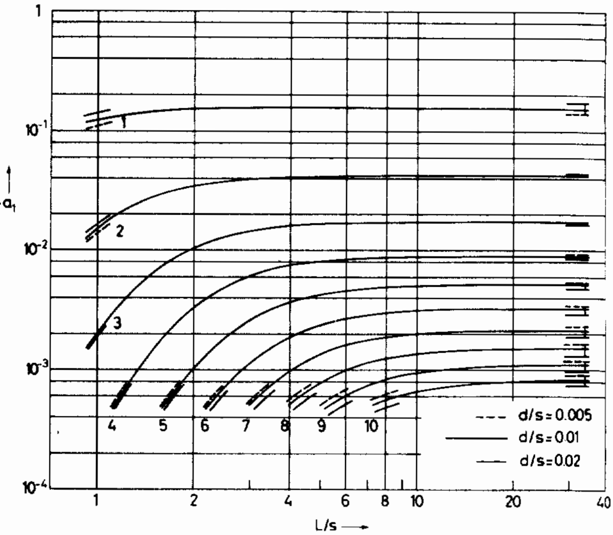


Fig. 4. Charge perturbations for displacements $\Delta x + i\Delta y$ of wire 0 in a symmetric chamber. Coefficients $a_1$ (negative for $j \geqslant 1$), where $(\Delta q_j/Q) = a_1(\Delta x/s) + a_2(\Delta x/s)^2 + b_2(\Delta y/s)^2 + \ldots$.

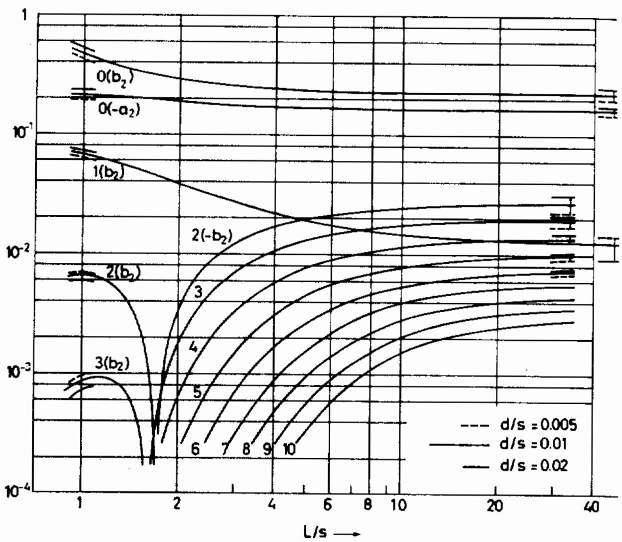


Fig. 5. Charge perturbations for displacements $\Delta x + i\Delta y$ of wire 0 in a symmetric chamber. Coefficients $a_2$ ($j = 0$ only) and $b_2$, where $(\Delta q_j/Q) = a_1(\Delta x/s) + a_2(\Delta x/s)^2 + b_2(\Delta y/s)^2 + \ldots$. Note that $a_2(j = 0)$ is negative and that $b_2(j \geqslant 2)$ changes sign near $L/s = 1.7$.

short segments indicating $d/s = 0.005$ and $d/s = 0.02$. It is interesting to note that for $j \geq 2$ the coefficient $b_2$ vanishes when $L/s$ has a value close to 1.7, the position of this zero being almost independent of $j$. Thus, for $L/s \approx 1.7$ the charges on wires other than 0 and 1 are almost unaffected by perpendicular displacements of wire 0.

Fig. 6 shows, for a particular symmetric chamber ($L/s = 4$, $d/s = 0.01$), the loci of displacements of wire 0 which correspond to a one per cent charge perturbation on wires 0, 1, 2. The shaded region is that to which the displacement must be restricted if *none* of these perturbations is to exceed one per cent. The corresponding region for a 0.1% perturbation would be reduced in width by a factor of 0.1, but in height by a factor of only $(0.1)^{\frac{1}{2}} = 0.32$.

## 5. Field plotting

The complex potential corresponding to any of the configurations discussed above can be written as

$$w(z) = \psi(z) + \sum_{j=-\infty}^{\infty} \Delta q_j \phi(z, z_j) + \\ + (Q + \Delta q_0)[\phi(z, z_0 + \Delta z) - \phi(z, z_0)],$$

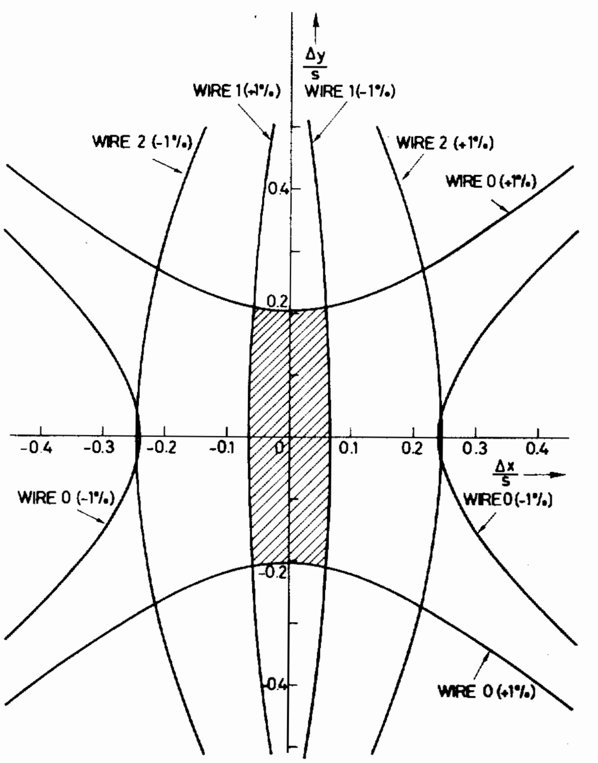


**Fig. 6. Displacements $\Delta x + i\Delta y$ of wire 0 which cause a $\pm 1\%$ charge perturbation on wires 0, 1, 2 of a symmetric chamber. $L/s = 4$, $d/s = 0.01$.**

where $\phi$ is defined by eq. (1), $\psi$ by eq. (3) or (5), and where the $\Delta q_j$, if non-zero, are calculated by the methods described in sections 2, 3 and 4 above. Equipotentials of this field, considered as functions of arc length $\sigma$, are given by

$$\frac{dz}{d\sigma} = -i \frac{\overline{w'(z)}}{|w'(z)|},$$

and field lines by

$$\frac{dz}{d\sigma} = -\frac{\overline{w'(z)}}{|w'(z)|},$$

where $w'(z)$ is obtained by analytical differentiation of $w(z)$.

Each of these differential equations may be replaced by a pair of simultaneous equations in $x$ and $y$ which can be integrated numerically by a standard technique such as the Runge–Kutta method (ref. 5, p. 212). Starting points for the integration of the field lines may be taken at equally spaced points on the surface of each wire. Starting points for the equipotentials must be obtained by inverse interpolation along some search line (e.g. a vertical line passing through the centre of each wire); but precautions must then be taken to avoid the repeated tracing of the same equipotential. In order to reduce the amount of calculation, a much larger integration step may be used in the neighbourhood of the electrodes, where both the equipotentials and the field lines are nearly straight, than in the neighbourhood of the wires, where the curvature is large.

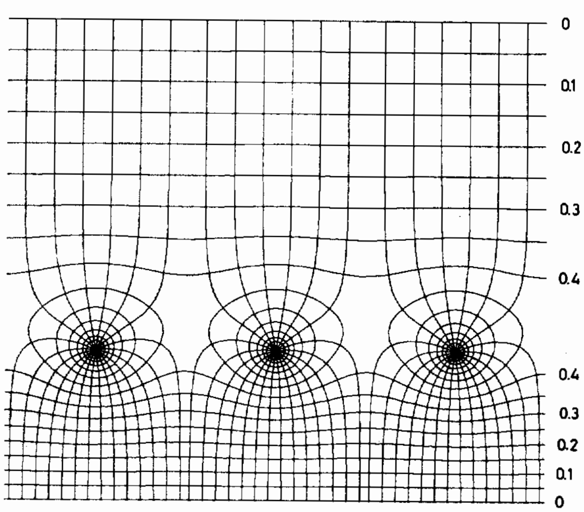


**Fig. 7. Field in a chamber with an unsymmetrically-placed grid at unit potential.**

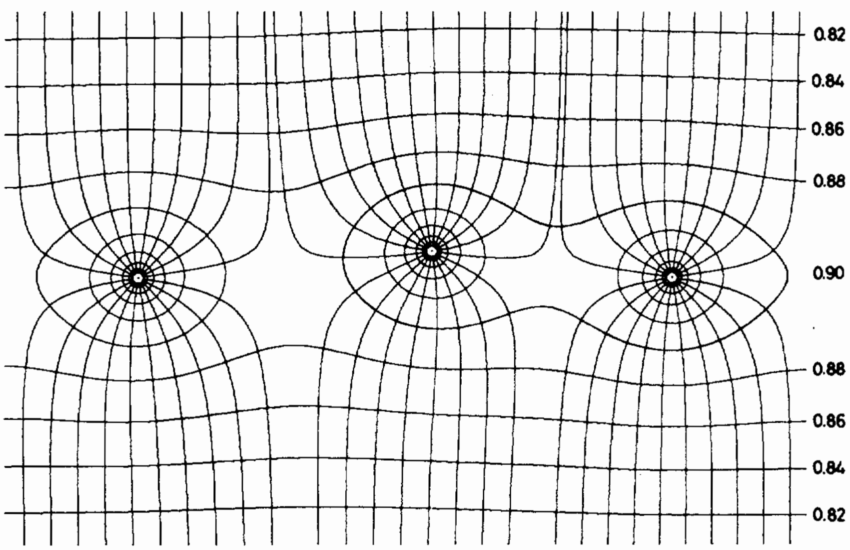


Fig. 8. Central portion of the field in a symmetrical chamber with one displaced wire. All wires at unit potential. $L/s = 8$, $d/s = 0.04$, $(\Delta x/s) = (\Delta y/s) = 0.1$.

As a check on the accuracy of the calculation it is advisable to recompute every $N$th point ($N = 5$ or $N = 10$) by inverse interpolation, and to restart the calculation at the exact point found in this way. To avoid difficulties during the inverse interpolation of field lines $\mathrm{Im}(w) = \text{constant}$, the cuts in the complex plane arising from the logarithmic terms in $\psi(z)$ and $\phi(z, z_j)$ should be chosen in such a direction as not to intersect the field line which is being currently integrated. Provision should also be made for the correct tracing of those solution curves which leave the specified rectangular plotting window only to re-enter it subsequently.

Parameters which must be supplied to the plotting program include: 1) the values of $\mathrm{Re}(w)$ and $\mathrm{Im}(w)$ which identify the equipotentials and field lines to be plotted, 2) a scale factor which indicates the magnification required, and 3) the dimensions of the plotting window. Two examples of such computer-generated plots are shown in figs. 7 and 8.

I should like to thank Prof. G. Charpak and Dr. F. Sauli for helpful discussions.

## Appendix

*Solution of discrete convolution equations.* Given adequately convergent real sequences $\{a_j\}$ and $\{c_j\}$, $-\infty < j < +\infty$, the problem is to find a finite number of terms of the infinite sequence $\{u_j\}$ which satisfies

$$\sum_{j=-\infty}^{\infty} a_{k-j} u_j = c_k, \quad -\infty < k < +\infty. \tag{11}$$

Eq. (7) is already in this form, and it will be shown below that the eqs. (10) can also be reduced to this form.

Using bold-faced letters to denote sequences, and the symbol $*$ to denote the discrete convolution operator, eq. (11) may be written as

$$\boldsymbol{a} * \boldsymbol{u} = \boldsymbol{c}.$$

It can easily be verified that the convolution operator is commutative and associative, i.e. that for any sequences $\boldsymbol{a}$, $\boldsymbol{b}$, $\boldsymbol{c}$,

$$\boldsymbol{a} * \boldsymbol{b} = \boldsymbol{b} * \boldsymbol{a},$$

$$\boldsymbol{a} * (\boldsymbol{b} * \boldsymbol{c}) = (\boldsymbol{a} * \boldsymbol{b}) * \boldsymbol{c}.$$

If $\boldsymbol{\delta}$ is the 'unit sequence' whose $j$th term is $\delta_{j0}$, then $\boldsymbol{\delta} * \boldsymbol{a} = \boldsymbol{a} * \boldsymbol{\delta} = \boldsymbol{a}$ for any $\boldsymbol{a}$, and the inverse $\boldsymbol{a}^{-1}$ of $\boldsymbol{a}$ may be defined by $\boldsymbol{a} * \boldsymbol{a}^{-1} = \boldsymbol{a}^{-1} * \boldsymbol{a} = \boldsymbol{\delta}$.

We now associate with the sequence $\{a_j\}$ the function $A(x)$ defined by the Fourier series

$$A(x) = \sum_{m=-\infty}^{\infty} a_m \mathrm{e}^{\mathrm{i}mx},$$

with analogous definitions for functions $U(x)$ and $C(x)$ associated with the sequences $\{u_j\}$ and $\{c_j\}$ respectively. It may then be verified that the sum on the left-hand side of eq. (11) is the coefficient of $\mathrm{e}^{\mathrm{i}kx}$ in the Fourier expansion of the product of $A(x)$ and $U(x)$. Thus eq. (11) is equivalent to

$$A(x)\,U(x) = C(x).$$

Hence,

$$U(x) = \sum_{k=-\infty}^{\infty} u_k e^{ikx} = \frac{C(x)}{A(x)}.$$

In particular, if $c = \delta$, then $U(x) = 1/A(x)$. Provided that $A(x)$ has no zeros in the interval $[0, 2\pi]$,

$$u_k = \frac{1}{2\pi}\int_0^{2\pi} e^{-ikx}\, U(x)\,dx. \tag{12}$$

Since $U(x)$ and all its derivatives are continuous and periodic in $[0, 2\pi]$, the integral (12) may be accurately approximated by the trapezoidal rule. Dividing the interval $[0, 2\pi]$ into $2N$ equal sub-intervals, and writing

$$U(x) = U_R(x) + iU_I(x),$$

(where $U_R$ is symmetric in $x$ and $U_I$ is antisymmetric on account of the reality of $c_k$ and $a_k$) we obtain

$$u_k \approx \frac{1}{N}\sum_{j=0}^{N}{}'' \left[U_R(j\alpha)\cos jk\alpha + U_I(j\alpha)\sin jk\alpha\right], \tag{13}$$

where $\alpha = \pi/N$ and where the double prime indicates that the terms corresponding to $j = 0$ and $j = N$ are to be taken with weight one half. The error of the approximation (13) is almost exactly equal (ref. 5, p. 278) to $u_{k-2N}$, and can be made negligible by choosing $N$ sufficiently large.

With $a_m$ defined by eq. (8) the requirement that $A(x)$ should be non-zero over $[0, 2\pi]$ is always satisfied; in fact it may be shown that in this case $A(x)$ is strictly positive for $d/L \le 8/\pi$.

*Convolution equations for finite displacements of a wire.* It was shown in section 4 that the finite displacement of a single wire leads to a system of eqs. (10) which is not of the form (11) directly soluble by the present method. These equations may, however, be reduced to this form.

If $\boldsymbol{f}$ is the sequence $\{f_k\}$, and if $\boldsymbol{f}'$ is the reversed sequence $\{f_{-k}\}$, the inner product occurring on the right-hand side of eq. (10) can be written as the zeroth term of a sequence formed by convolution:

$$\sum_{j=-\infty}^{\infty} u_j f_j = (\boldsymbol{u} * \boldsymbol{f}')_0.$$

On defining

$$g = \sum_{j=-\infty}^{\infty} f_j,$$

the eqs. (10) become

$$\boldsymbol{a} * \boldsymbol{u} = (1+u_0)\boldsymbol{f} + [g - (1+u_0)f_0 + (\boldsymbol{u} * \boldsymbol{f}')_0]\boldsymbol{\delta},$$

i.e.

$$\boldsymbol{u} = \lambda(\boldsymbol{a}^{-1} * \boldsymbol{f}) + \mu \boldsymbol{a}^{-1}, \tag{14}$$

where

$$\lambda = 1 + u_0,$$

$$\mu = g - \lambda f_0 + (\boldsymbol{u} * \boldsymbol{f}')_0. \tag{15}$$

Hence,

$$(\boldsymbol{u} * \boldsymbol{f}')_0 = \lambda(\boldsymbol{a}^{-1} * \boldsymbol{f} * \boldsymbol{f}')_0 + \mu(\boldsymbol{a}^{-1} * \boldsymbol{f}')_0.$$

Provided $z_0$ is on the $y$-axis, $a_{-m} = a_m$ and hence $(\boldsymbol{a}^{-1} * \boldsymbol{f}')_0 = (\boldsymbol{a}^{-1} * \boldsymbol{f})_0$. Therefore, on defining $\boldsymbol{r}$, $\boldsymbol{s}$ and $\boldsymbol{t}$ by

$$\boldsymbol{a} * \boldsymbol{r} = \boldsymbol{\delta}, \quad (\text{i.e. } \boldsymbol{r} = \boldsymbol{a}^{-1}) \tag{16}$$

$$\boldsymbol{a} * \boldsymbol{s} = \boldsymbol{f}, \tag{17}$$

$$\boldsymbol{a} * \boldsymbol{t} = \boldsymbol{f} * \boldsymbol{f}', \tag{18}$$

we obtain

$$(\boldsymbol{u} * \boldsymbol{f}')_0 = \lambda t_0 + \mu s_0. \tag{19}$$

Equating the zeroth component of eq. (14) to $u_0 = 1 - \lambda$, and using eqs. (15) and (19), yields the following simultaneous equations for $\lambda$ and $\mu$:

$$\begin{pmatrix} 1 - s_0 & -r_0 \\ f_0 - t_0 & 1 - s_0 \end{pmatrix}\begin{pmatrix} \lambda \\ \mu \end{pmatrix} = \begin{pmatrix} 1 \\ g \end{pmatrix}. \tag{20}$$

The computational procedure is as follows:

1) Using the method of the preceding section, solve eqs. (16) and (17) for as many terms of $\boldsymbol{r}$ and $\boldsymbol{s}$ as are needed in the final solution $\boldsymbol{u}$.
2) Solve eq. (18) for $t_0$, noting that the Fourier sum associated with $\boldsymbol{f} * \boldsymbol{f}'$ is merely $|F(x)|^2$.
3) Compute $\lambda$ and $\mu$ from eq. (20).
4) Compute $\boldsymbol{u} = \lambda \boldsymbol{s} + \mu \boldsymbol{r}$.

*Convolution equations for small displacements.* For small displacements $\Delta z = \Delta x + i\Delta y$ of wire 0 in a symmetric chamber, neglecting terms of order $|\Delta z|^3$,

$$\boldsymbol{f} = \boldsymbol{\alpha}_1(\Delta x/s) + \boldsymbol{\alpha}_2(\Delta x/s)^2 + (\rho^2\boldsymbol{\delta} - \boldsymbol{\alpha}_2)(\Delta y/s)^2, \tag{21}$$

where

$$\rho = \frac{\pi s}{2L}, \quad (\boldsymbol{\alpha}_1)_0 = (\boldsymbol{\alpha}_2)_0 = 0,$$

$$(\boldsymbol{\alpha}_1)_j = -\frac{2\rho}{\sinh(j\rho)}, \quad \text{for } j \ne 0,$$

$$(\boldsymbol{\alpha}_2)_j = -\rho^2 \frac{\cosh(j\rho)}{\sinh^2(j\rho)}, \quad \text{for } j \neq 0.$$

To the same order, the sequence $u_j = \Delta q_j/Q$ can be written as

$$\boldsymbol{u} = \boldsymbol{a}_1(\Delta x/s) + \boldsymbol{a}_2(\Delta x/s)^2 + \boldsymbol{b}_2(\Delta y/s)^2 , \tag{22}$$

where the subscripts distinguish sequences, not terms of sequences. Substituting eqs. (21) and (22) into eqs. (10), we obtain the following equations for $\boldsymbol{a}_1$, $\boldsymbol{a}_2$, $\boldsymbol{b}_2$:

$$\sigma = \sum_{j=-\infty}^{\infty} (\boldsymbol{\alpha}_2)_j ,$$

$$\boldsymbol{a} * \boldsymbol{t} = \boldsymbol{\alpha}_1 * \boldsymbol{\alpha}_1 , \quad \text{(only } t_0 \text{ is required)}$$

$$\boldsymbol{a} * \boldsymbol{a}_1 = \boldsymbol{\alpha}_1 ,$$

$$\boldsymbol{a} * \boldsymbol{a}_2 = (\sigma + t_0)\boldsymbol{\delta} + \boldsymbol{\alpha}_2 ,$$

$$\boldsymbol{a} * \boldsymbol{b}_2 = (\rho^2 - \sigma)\boldsymbol{\delta} - \boldsymbol{\alpha}_2 .$$

These convolution equations may be solved numerically by the method described above.

## References


1) G. Charpak, Ann. Rev. Nucl. Sci. **20** (1970) 195.

2) H. Buchholz, *Elektrische und magnetische Potentialfelder* (Berlin, 1957).

3) P. M. Morse and H. Feshbach, *Methods of theoretical physics*, Part 2 (New York, 1953) p. 1241.

4) E. T. Whittaker and G. N. Watson, *A course of modern analysis* (Cambridge, 1946) p. 464.

5) R. W. Hamming, *Numerical methods for scientists and engineers* (New York, 1962).